

Phase shift analysis of π^\pm - ^4He elastic scattering

B. Brinkmüller

Institut für Experimentelle Kernphysik, Universität Karlsruhe, 76128 Karlsruhe, Germany

H. G. Schlaile

Institut für Theoretische Teilchenphysik, Universität Karlsruhe, 76128 Karlsruhe, Germany

(Received 11 February 1993)

An energy-dependent phase shift analysis of π^\pm - ^4He elastic scattering data up to an energy $T_\pi = 260$ MeV was carried out. Using a careful treatment of Coulomb effects to describe the Coulomb nuclear interference we reexamined the constraints to the π - ^4He forward scattering amplitude f_0 by dispersion relations. This allows a stringent consistency check of the data. A satisfactory description of the data could only be achieved assuming large error bars of the total cross section measurements and allowing normalization factors for the differential cross section data.

PACS number(s): 25.80.Dj

I. INTRODUCTION

The π - ^4He system is one of the simplest pion nucleus systems and therefore very important for the test of pion nuclear scattering models. Several angular distributions of the π - ^4He elastic cross section have been measured by different groups [1–6] in the energy region from $T_\pi = 24$ to 260 MeV. From measurements of the differential cross section at forward angles one can extract the real part of the forward nuclear scattering amplitude f_0 , using Coulomb-nuclear interference. This was done by Binon *et al.* [5] and in a more sophisticated way, but with essentially the same results, by Das and Deo [7].

Several groups [8–10] have made dispersion relation analyses to calculate the real part of the forward scattering amplitude of this reaction starting from total cross section measurements. The cross section in this energy region is dominated by the Δ_{33} π -nucleon resonance at $T_\pi \approx 180$ MeV, close to which the real part of the forward amplitude goes through zero. It shows a maximum at $T_\pi \approx 100$ MeV and a minimum at $T_\pi \approx 300$ MeV. It was found that there exist discrepancies between dispersion relation calculations and measurements of the real part of the forward scattering amplitude at energies above the resonance, especially at $T_\pi = 260$ MeV, with $\text{Re}f_0(\text{measured}) > \text{Re}f_0(\text{calculated})$.

Recently, new data from π - ^4He elastic cross sections measurements at Los Alamos became available [11] spanning the energy range from $T_\pi = 90$ to 240 MeV and an angle range from 10° to 170° . Both π^+ and π^- data were taken with much reduced error bars in the large angle region, where the cross sections are small. Previously high quality data only existed for π^- - ^4He differential cross sections at forward angles [5]. The availability of both π^+ and π^- differential cross section data allows a better determination of $\text{Re}f_0$. In a first analysis [11] it was found that $\text{Re}f_0(\text{measured}) < \text{Re}f_0(\text{calculated})$ for energies below the resonance. However, in that analysis Coulomb effects were treated very roughly.

The disagreement with dispersion relation predictions is either due to inconsistencies in the existing data set, or

must have its origin in a wrong description of Coulomb or other charge symmetry breaking effects, that contribute to the difference of cross sections for π^+ and π^- scattering.

The origin of the problems can be investigated best in a phase shift analysis, that includes careful treatment of Coulomb effects and the dispersion relation. Such an analysis was made by Nichitiu *et al.* [12] before the Los Alamos data were available. They were able to find a solution without the disagreement at $T_\pi = 260$ MeV. However, in this solution, the slope of $\text{Im}f_0$ near threshold was incompatible with mesic atom data [13]. So, the problem was not solved, but only shifted.

We therefore made a phase shift analysis including the new data, along the line of earlier work on π^\pm - ^{12}C [14], π^\pm - ^{16}O [15], and π^\pm - ^{40}Ca [16]. In the analysis we used the forward dispersion relation as described by Pilkuhn *et al.* [13] to obtain the real part of the forward scattering amplitude from the imaginary part. In the following we give a short description of the formalism used to treat Coulomb effects (Sec. II) and the dispersion relation (Sec. III), before we compare the result of our analysis with the data (Sec. IV) and discuss remaining discrepancies (Sec. V).

II. COULOMB CORRECTIONS

The elastic differential cross section of π^\pm - ^4He scattering is described by

$$d\sigma^\pm/d\Omega = |f_{\text{tot}}^\pm|^2. \quad (1)$$

The total amplitude f_{tot}^\pm consists of a sum of three parts

$$f_{\text{tot}}^\pm = f_h + f_C^\pm + f_R^\pm. \quad (2)$$

f_h is the pure hadronic amplitude, f_C^\pm the pure Coulomb amplitude, and f_R^\pm represents the Coulomb corrections which take into account the modifications of the pure hadronic force by Coulomb effects [17]. f_C^\pm can be split into the part $f_C^{\text{point}\pm}$, where the pion and the ^4He nu-

cleus are treated as pointlike particles and $f_C^{\text{ext}\pm}$, which represents the contribution from the charge extension of π^\pm and ${}^4\text{He}$ to the Coulomb amplitude:

$$f_C^\pm = f_C^{\text{point}\pm} + f_C^{\text{ext}\pm}. \quad (3)$$

$f_C^{\text{ext}\pm}$ is calculated numerically with the ${}^4\text{He}$ form factor F_α of Germond and Wilkin [18] and the pion form factor F_π of Frosch [19] from the Klein-Gordon equation [14].

The differential cross section at very forward scattering angles is sensitive to relativistic effects in the point Coulomb amplitude. Therefore we use the very accurate formula [20, 21]

$$f_C^{\text{point}} = f_C^{(0)} + f_C^{(1)} + \Delta f_C^{(1)} \quad (4)$$

where

$$f_C^{(0)} = -\frac{\eta}{2k \sin^2\left(\frac{1}{2}\Theta\right)} e^{-i\eta \ln \sin^2\left(\frac{1}{2}\Theta\right) + 2i\sigma_0}, \quad (5)$$

$$f_C^{(1)} = f_C^{(0)} \left(-\frac{1}{2} \pi \eta v_{lab}^2 \sin\left(\frac{1}{2}\Theta\right) e^{2i\sigma_{-1/2} + 2i\sigma_0} \right), \quad (6)$$

$$\Delta f_C^{(1)} = -\sum_{l=0}^L f_{C,l}^{(1)} + \frac{1}{2ik} \sum_{l=0}^L (2l+1) (e^{2i\sigma_\gamma} - e^{2i\sigma_l}) P_l. \quad (7)$$

η is the Sommerfeld parameter, $\gamma = [(l + \frac{1}{2})^2 - z^2 \alpha^2]^{1/2}$ with $z = 2$ and $\alpha = 1/137$. σ is given by

$$e^{2i\sigma_l} = \frac{\Gamma(\bar{l} + 1 + i\eta)}{\Gamma(\bar{l} + 1 - i\eta)}, \quad (8)$$

$$e^{2i\sigma_\gamma} = e^{-i\pi(\gamma-1/2-l)} \frac{\Gamma(\gamma + 1/2 + i\eta)}{\Gamma(\gamma + 1/2 - i\eta)} \quad (9)$$

where \bar{l} is either $-1/2$ or l .

The fact that negative pions are accelerated towards the nucleus while positive pions are slowed down changes not only the momentum of the pions but also their impact parameter. This is taken into account with the last contribution f_R^\pm to Eq. (2). After a partial wave decomposition, the amplitude f_{tot}^\pm can be expressed in terms of real and imaginary phase shifts δ^\pm and ω^\pm :

$$f_{\text{tot},l}^\pm = \frac{1}{2ik} \left(e^{2i(\delta_{\text{tot},l}^\pm + i\omega_{\text{tot},l}^\pm)} - 1 \right). \quad (10)$$

We calculate the Coulomb corrections in terms of these phase shifts [14]

$$\delta_{R,l}^\pm = \delta_{\text{tot},l}^\pm - \delta_{h,l} - \delta_{C,l}^\pm, \quad (11)$$

$$\omega_{R,l}^\pm = \omega_{\text{tot},l}^\pm - \omega_{h,l}, \quad (12)$$

with

$$\delta_{R,l}^\pm = \hat{\alpha}_l^\pm (d\delta_{h,l}/dk + \sin 2\delta_{h,l} \cosh 2\omega_{h,l}/2k), \quad (13)$$

$$\omega_{R,l}^\pm = \hat{\alpha}_l^\pm (d\omega_{h,l}/dk + \cos 2\delta_{h,l} \sinh 2\omega_{h,l}/2k). \quad (14)$$

With the Coulomb factors

$$\hat{\alpha}_l^\pm = \pm \frac{2m_\pi z \alpha k}{\pi} \times P \int_0^\infty dk' \frac{k'^2}{k^2 - k'^2} \int_{-1}^1 dx \frac{P_l(x) F_\alpha(q^2) F_\pi(q^2)}{q^2}, \quad (15)$$

where m_π is the pion mass and q is the transferred momentum. As not only the hadronic phases $\delta_{h,l}$ and $\omega_{h,l}$ but also their derivatives $d/dk\delta_{h,l}$ and $d/dk\omega_{h,l}$ are needed for the calculation of the cross section, this formalism can only be used in an energy-dependent analysis.

III. DISPERSION RELATION

For the crossing symmetric hadronic amplitude f_h the once subtracted dispersion relation reads

$$\text{Re} f_h(k^2, t=0) = \text{Re} f_h(m_\pi) + \sum_i \frac{2\omega_i f_i^2 k^2}{(\omega^2 - \omega_i^2) k_i^2} + \frac{2k^2}{\pi} P \int_{\omega_n}^\infty \frac{\omega' d\omega'}{k'^2} \frac{\text{Im} f_h}{\omega'^2 - \omega^2}, \quad (16)$$

where $f_h(m_\pi) = A_0 = (-0.138 + 0.045i)$ fm [22] is the complex scattering length at $T_\pi = 0$ MeV and the pole sum represents the contribution from excited nuclear states. The lower limit of the integrand is the nucleon emission threshold ω_n . For the threshold expansion of $\text{Im} f_h$ we follow the procedure of Pilkuhn *et al.* [13] and divide it into three pieces

$$\text{Im} f_h = \text{Im}_I f_h + \text{Im}_{II} f_h + \text{Im}_{eI} f_h, \quad (17)$$

where $\text{Im}_I f_h$ comes from pion absorption on one nucleon, $\text{Im}_{II} f_h$ from two or more nucleon absorption, and $\text{Im}_{eI} f_h$ from elastic π -nuclear scattering. As $\text{Im}_I f_h$ is negligible throughout the physical region, it is sufficient to combine the dispersion integral over it with the poles into a single effective pole $f_{\text{eff}}^2/(\omega^2 - \omega_{\text{eff}}^2)$. Assuming moreover $\omega_{\text{eff}}^2 \ll \omega^2$, $k_n^2 \approx -m_\pi^2$ we obtain

$$\text{Re} f_h(k^2, t=0) = \text{Re} A_0 - \frac{2k^2}{m_\pi^2 \omega^2} \omega_{\text{eff}} f_{\text{eff}}^2 + \frac{2k^2}{\pi} P \int_{\omega_{nn}}^\infty \frac{\omega' d\omega'}{k'^2} \frac{\text{Im} f_h - \text{Im}_I f_h}{\omega'^2 - \omega^2} \quad (18)$$

where the lower limit for the integration is now the ${}^4\text{He}$ binding energy $\omega_{nn} = 28.3$ MeV, which we prefer to use instead of twice the neutron emission threshold used by Pilkuhn *et al.* [13]. The magnitude of the effective pole is not well determined theoretically, but its contribution to $\text{Re} f_0$ is believed to be small. Values of $\omega_{\text{eff}} f_{\text{eff}}^2 = 0$ to -6.4 MeV have been used before [9, 13, 23]. We determined $\omega_{\text{eff}} f_{\text{eff}}^2$ by a fit to the data and also investigated the effect of changing this parameter on the different data sets (see Sec. V).

To estimate the contribution of the integral close to threshold we use the threshold expansion [13]

$$f_{\text{thr exp}} = \frac{A_0 + k^2 B_0}{1 - ik(A_0 + k^2 B_0)} + \frac{3k^2}{1/A_1 - ik^3} \quad (19)$$

with

$$\begin{aligned} B_0 &= -0.18 \text{ fm}^3, \\ A_1 &= (0.42 + 0.06i) \text{ fm}^3. \end{aligned}$$

Because the dominating contribution to the scattering amplitude at threshold comes from two nucleon absorption, we multiply $f_{\text{thr exp}}$ with the approximate phase space factor for this reaction to obtain

$$\text{Im}f_h - \text{Im}_I f_h = \frac{\omega - \omega_{nn}}{m_\pi - \omega_{nn}} \text{Im}f_{\text{thr exp}}. \quad (20)$$

This threshold expansion is used up to an energy of $T_\pi = 20$ MeV where inelastic π - ^4He scattering starts to contribute.

IV. THE HADRONIC AMPLITUDE

The general features of the angular distribution of the differential cross sections of π - ^4He scattering up to an energy of $T_\pi = 260$ MeV can be well described by an exponential decrease from the cross section at $\Theta = 0^\circ$ and one or two minima at larger angles. Therefore an often used ansatz for the description of the pure hadronic amplitude is

$$f_h(k, t) = f_0(k) e^{B(k)t} \prod_{i=1}^2 [1 - t/t_i(k)] \quad (21)$$

with $t = -2k^2(1 - \cos \Theta)$, where k and Θ are the c.m. momentum and scattering angle, respectively. The form contains B , a real function of k , and three complex functions of k , namely the forward scattering amplitude f_0 and t_i , that describe the cross section near the first and possible second minimum. For the energies discussed here, a possible third zero would be located beyond the backward direction in the unphysical region and only affect the slope, but cannot give more structure for the fit. To be able to use this ansatz together with the Coulomb corrections described in the previous section, a Legendre decomposition of the hadronic amplitude is made to obtain the hadronic phases.

An advantage of this ansatz is the explicit occurrence of f_0 as a parameter. This allows a simple algorithm to include the forward dispersion relation to calculate $\text{Re}f_0$ from $\text{Im}f_0$. This way the constraints given by dispersion relation and unitarity are satisfied and we do not rely on separate measurements of the real and imaginary part of the forward scattering amplitude.

Analytic expressions for B , $\text{Im}f_0$, and t_i were chosen to describe the energy dependence of the hadronic amplitude. The expression for $\text{Im}f_0$ was required to join smoothly to values for $\text{Im}f_0$ obtained from total cross section data of Chavanon *et al.* [24], which span an energy range from $T_\pi = 465$ to 1160 MeV. For higher energies, the parametrization [23, 9]

$$\sigma^{\text{tot}} = \sigma^\infty + \sqrt{\frac{B_a}{\omega}} \quad (22)$$

is used with $\sigma^\infty = 0.071$ b and $B_a = 4.79$ MeV b². This formula reproduces well the total cross section measured for $k = 3.48$ GeV/c and 6.13 GeV/c [25], $k = 7.76$ GeV/c [26], and $k = 40.4$ GeV/c [27]. In contrast, differential cross sections measured at $k = 5$ GeV/c [28] give a forward scattering amplitude about a factor of 2 too low when extrapolated to $\Theta = 0^\circ$. As there are also problems to reproduce the forward part of this angular distribution by theoretical calculations [28, 29], we believe that there is a normalization problem at least with part of these data. Total cross sections measured for energies above 40 GeV show a slight increase [30] with energy. Using a logarithmic increase of the cross section to reproduce these data changes the results of the dispersion calculations by less than 0.001 fm for the real part of the forward scattering amplitude at energies below 300 MeV (see Fig. 2).

To determine the coefficients of the expressions for B , t_i , and $\text{Im}f_0$, we used differential cross section measurements from Nordberg and Kinsey [1] at $T_\pi = 24$ MeV, Fournier *et al.* [6] at $T_\pi = 25$ and 51 MeV, Block *et al.* [2] at $T_\pi = 51$ –68 MeV, Crowe *et al.* [3] at $T_\pi = 51$ –75 MeV, Brinkmüller *et al.* [11] at $T_\pi = 90$ –240 MeV, and Binon *et al.* [5] at $T_\pi = 110$ –260 MeV. In the energy region from 260 to 465 MeV there exist only the measurements of the elastic cross section by Boswell *et al.* [31], which are not complete enough to be used in a phase shift analysis. Therefore $\text{Im}f_0$ is only determined by interpolation in this energy interval. Assuming a smooth interpolation from 260 to 465 MeV only little freedom is left. Even when using rather large or small values for $\text{Im}f_0$ in this energy interval no significant improvement of the description at $T_\pi = 240$ and 260 MeV can be obtained.

We also used total cross section data from Block *et al.* [2] at $T_\pi = 51$ –68 MeV, Johnson [32] at $T_\pi = 51$ –105 MeV, Binon *et al.* [5] at $T_\pi = 110$ MeV, and Wilkin *et al.* [8] at $T_\pi = 110$ –262 MeV. There are large systematic uncertainties due to Coulomb corrections, and the discrepancies between data taken by different groups exceed the quoted error bars by far. Therefore, we only included data from groups that measured both π^+ and π^- cross sections and used the average of this. By this we made sure that at least to first order differences in the treatment of Coulomb effects used for the extraction of the total nuclear cross sections cancel. Furthermore we assumed a 10% error for all these measurements independent from the quoted errors. The absolute normalization of the differential cross section data sets was treated on the same basis as the total cross section data, assuming also a 10% error.

As the number of data points for energies above 90 MeV by far exceeds the number of data points at lower energies, we did not minimize the overall χ^2 , but calculated χ^2 per number of data points individually for each energy where data exist. We then minimized the function

$$f = \sum_{i=1}^{n_e} \chi_e^2 / n_e + \sum_{i=1}^{n_t} \chi_t^2 / n_t, \quad (23)$$

where n_e is the number of energies where differential elastic scattering data exist and n_t is the number of total

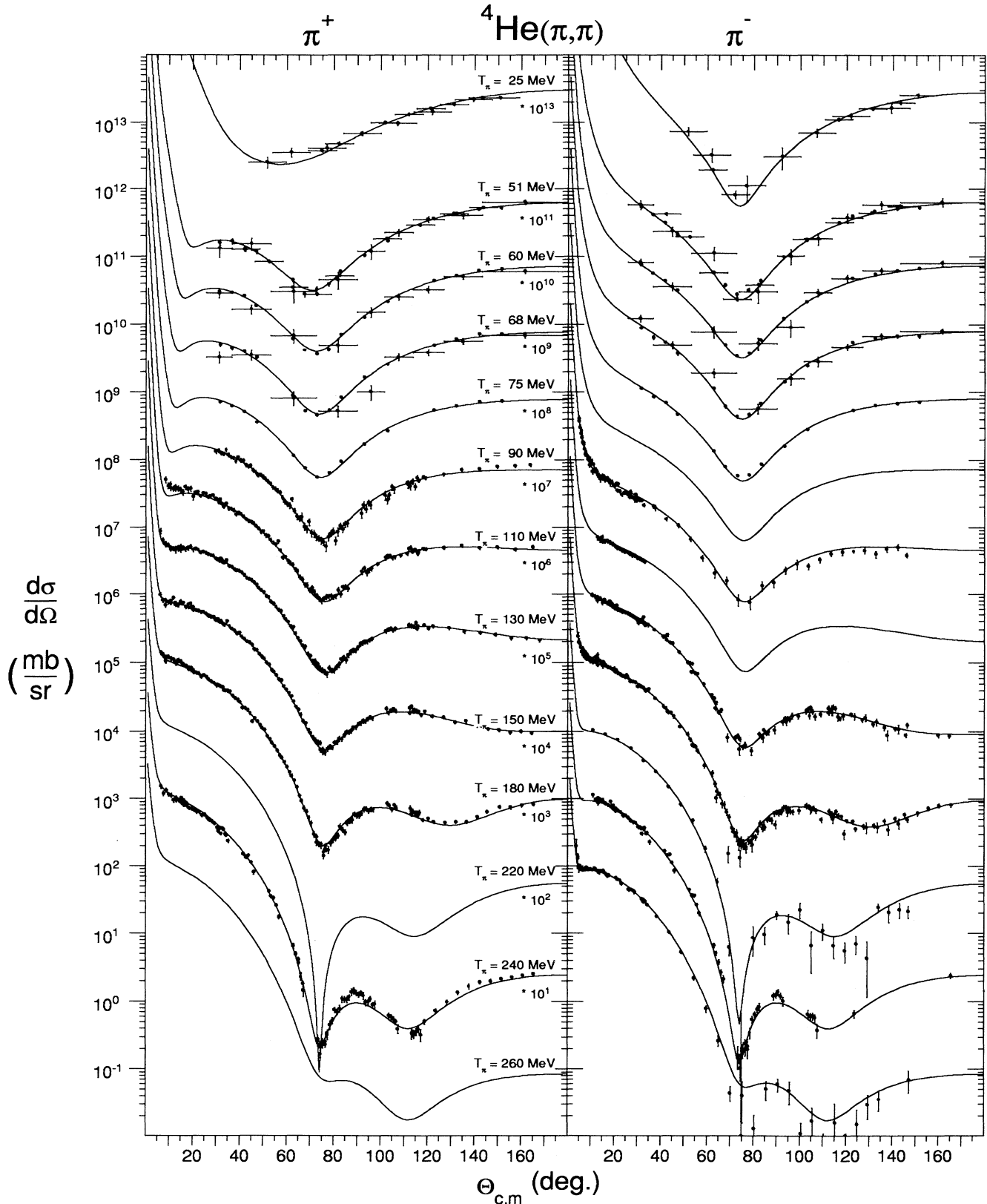


FIG. 1. Summary of π - ${}^4\text{He}$ elastic differential cross section measurements. The data points are from Nordberg and Kinsey [1], Fournier *et al.* [6], Block *et al.* [2], Crowe *et al.* [3], Brinkmøller *et al.* [11], and Binon *et al.* [5]. Data at $T_\pi = 24$ MeV are plotted together with data at 25 MeV, data at $T_\pi = 58$ MeV together with data at 60 MeV, and data at $T_\pi = 65$ MeV together with data at 68 MeV. For the fit the correct energies were used.

TABLE I. Normalization factors and χ^2 per number of data points (N_{dp}) obtained in our energy-dependent analysis. The value in brackets for χ^2/N_{dp} was obtained when keeping all normalization factors equal to 1.

T_π (MeV)	Reference	N_{dp}	norm.	χ^2/N_{dp}
24.1	[1]	15	0.94	1.28 (1.60)
25.1	[6]	12	1.05	1.63 (2.62)
51.0	[6]	18	1.05	8.55 (11.10)
51.0	[3]	30	1.04	2.32 (4.58)
51.0	[2]	18	0.83	0.86 (3.55)
58.0	[2]	18	0.85	1.25 (5.21)
60.0	[3]	30	1.13	7.20 (8.42)
65.0	[2]	18	0.78	2.25 (7.86)
68.0	[3]	30	1.22	2.10 (5.92)
75.0	[3]	30	1.20	4.55 (11.29)
90.0	[11]	81	0.94	1.28 (4.80)
110.0	[11]	134	0.93	2.04 (4.86)
110.0	[5]	64	1.07	2.37 (2.36)
130.0	[11]	143	0.93	0.89 (2.51)
150.0	[11]	211	0.93	1.43 (2.24)
150.0	[5]	30	0.98	2.01 (1.87)
180.0	[11]	230	0.98	1.57 (1.56)
180.0	[5]	59	1.03	5.62 (7.54)
220.0	[5]	27	0.98	2.53 (2.51)
240.0	[11]	193	1.16	2.71 (6.13)
260.0	[5]	61	0.98	3.61 (10.19)

cross section measurements plus the number of differential cross section data sets. χ_e^2 is the χ^2 per number of data points for the differential cross section data and χ_t^2 is the χ^2 from the total cross section data and the absolute normalization of the differential cross section data. For the minimization we used the computer code MINUIT [33]. With the coefficients of the expressions for $\text{Im}f_0$, B , t_i , and $\omega_{\text{eff}}f_{\text{eff}}^2$ we had 27 parameters to fit 15 data points for the total cross section and 1448 data points for differential cross sections in 21 different data sets.

Table I shows the normalization factors used for the different data sets and the obtained χ^2 . In Fig. 1 the

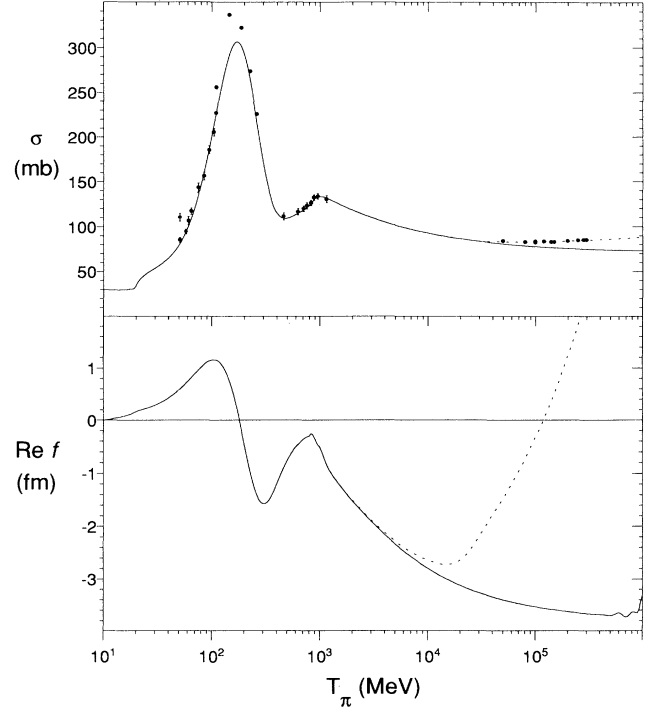


FIG. 2. The upper part shows the total cross section obtained from the fit. The data are from Block *et al.* [2], Johnson [32], Binon *et al.* [5], Wilkin *et al.* [8], Chavanon *et al.* [24], and Burq *et al.* [30]. The lower part shows the real part of the forward scattering amplitude obtained from this by dispersion relation. The influence of a logarithmic increase in the total cross section to fit the data of Burq *et al.* (dashed curve) is only noticeable for energies above 1 GeV. So it was not used in this analysis.

angular distributions obtained by the fit are compared to the data. Table II shows the total cross section measurements used together with total cross sections from the fit. Figure 2 shows the fit to the total cross section data and $\text{Re}f_0$ that is calculated from it with the help of

TABLE II. Total and total elastic cross sections from the analysis. The total cross sections are compared to measurements of different groups. The experimental result is in each case the average of the measured π^+ and π^- total cross sections.

T_π (MeV)	Reference	σ_{tot} (exp.)	σ_{tot} (fit)	σ_{el} (fit)
51.0	[2]	85.2 ± 2.9	81.2	29.6
51.0	[32]	110.5 ± 4.3	81.2	29.6
58.0	[2]	94.7 ± 2.7	94.1	36.5
61.0	[32]	106.8 ± 4.3	100.3	39.7
65.0	[2]	117.2 ± 3.6	109.0	44.0
75.0	[32]	143.2 ± 5.2	133.3	54.9
85.0	[32]	156.2 ± 4.5	159.9	65.2
95.0	[32]	185.7 ± 4.5	187.4	74.6
105.0	[32]	205.5 ± 4.2	214.2	83.0
110.0	[5]	227.2 ± 1.4	227.0	87.2
110.0	[8]	256.0 ± 2.0	227.0	87.2
146.0	[8]	336.0 ± 1.0	293.4	105.0
189.0	[8]	322.0 ± 1.0	300.8	109.0
225.0	[8]	274.0 ± 1.0	264.5	98.9
262.0	[8]	226.0 ± 1.0	215.3	82.0

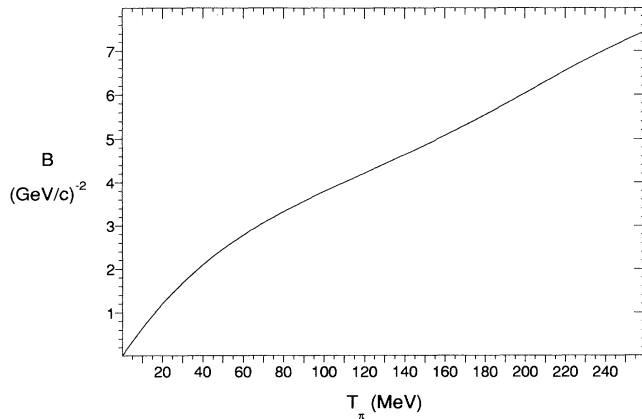


FIG. 3. The slope parameter B as a function of pion kinetic energy.

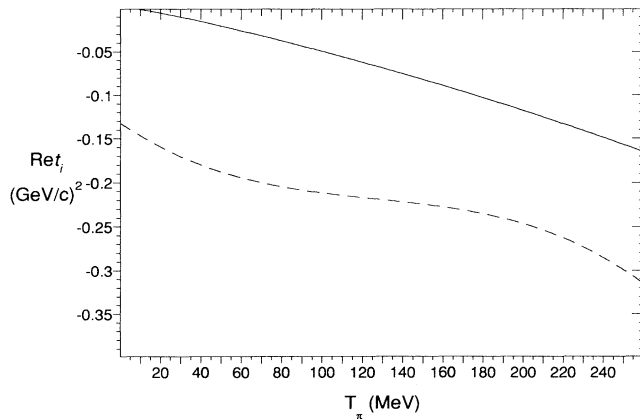


FIG. 4. The real part of the first (solid line) and second (dashed line) zero of the hadronic amplitude as a function of pion kinetic energy.

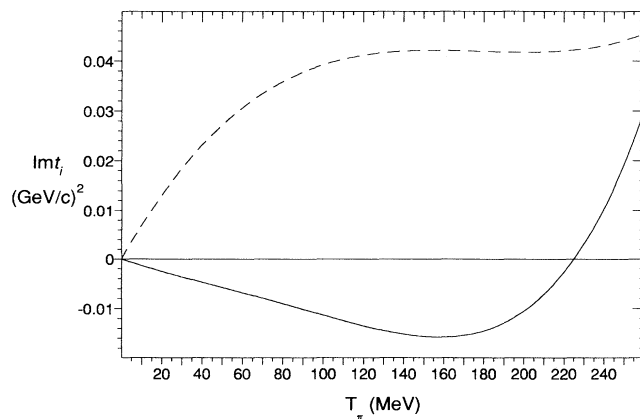


FIG. 5. The imaginary part of the first (solid line) and second (dashed line) zero of the hadronic amplitude as a function of pion kinetic energy.

the dispersion relation. As can be seen from Figs. 3–5 the variation with energy of the slope parameter B and of t_i is very smooth. The general behavior of the parameters is very similar to that found by Binon *et al.* [5]. However, we use a different sign convention for t_i and for $\text{Im}t_1$ we prefer a solution with a change of sign at about $T_\pi = 225$ MeV.

In the fit we obtained a value of $\omega_{\text{eff}} f_{\text{eff}}^2 = -6$ MeV, which is within the range of values obtained before. However, this result depends strongly on the way the weight of the total cross section data is chosen in the fit. So we cannot claim to be able to determine the contribution of the pole term accurately.

V. DISCUSSION OF RESULTS

For energies where both π^+ and π^- have been measured, we can compare our solution to experimental results for the charge asymmetry $A = \frac{\sigma_{-}^{-} - \sigma_{+}^{+}}{\sigma_{-}^{-} + \sigma_{+}^{+}}$ (Fig. 6). The agreement with the data is very good. Larger discrepancies only exist for the forward angle data at $T_\pi = 110$ MeV, which are discussed below. We conclude that our treatment of Coulomb effects as the only origin of charge symmetry breaking is adequate. A similar conclusion was already drawn by Khankhasayev *et al.* [34] using data below the Δ_{33} resonance only. Here we can show the nice agreement obtained also for resonance energies ($T_\pi = 180$ MeV) in the minimum of the angular

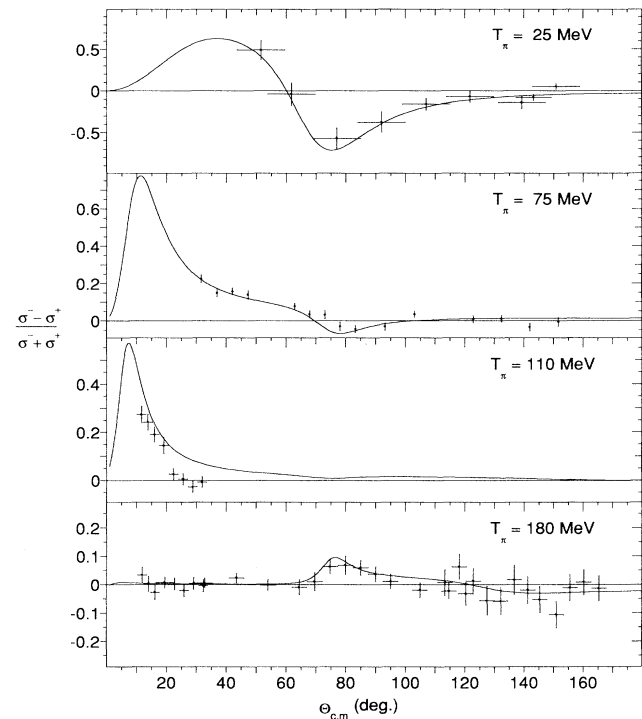


FIG. 6. The charge asymmetry $A = \frac{\sigma_{-}^{-} - \sigma_{+}^{+}}{\sigma_{-}^{-} + \sigma_{+}^{+}}$ for various energies. With the exception of $T_\pi = 110$ MeV a reasonable description of the data is achieved. Unfortunately there exist no measurements close to the maximum of A at forward angles below an energy of $T_\pi = 110$ MeV.

distribution. This is in contrast to the preliminary result of Brinkmüller *et al.* [11], who obtained the wrong sign for A at this energy and angle.

In the preliminary analysis the real parts of the nuclear phases δ_l and the absorption coefficients η_l were used as fit parameters. In several calculations we checked whether the differences to this preliminary analysis were due to the different treatment of Coulomb effects or to differences in the parametrization of the nuclear amplitude. Using η_l and δ_l as fit parameters and our treatment of Coulomb corrections in an energy-dependent analysis over a limited energy interval we could improve the overall χ^2 with respect to the results obtained by Brinkmüller *et al.* and obtained the measured sign of A at $T_\pi = 180$ MeV. This shows the importance of a good description of the Coulomb part.

We also obtained a better χ^2 than for the results presented here. This is due on one side to the increased number of parameters that lead to a better description of the large angle region at higher energies. On the other side, the results obtained using η_l and δ_l do not satisfy the dispersion relation, which constrains our forward angle scattering amplitude.

Therefore we think that, in spite of the unsatisfactory χ^2 obtained in our analysis, it is a good basis to discuss possible inconsistencies in the existing data. For each data set we examined the reason for possible deviations from the fit and investigated how a better description of a particular data set would affect the rest of the data.

For the lowest energies the forward angle cross sections for π^- - ^4He at $T_\pi = 51$ MeV measured by Crowe *et al.* [3] and by Fournier *et al.* [6] are incompatible with each other. Our solution follows the data of Crowe *et al.* To fit the data of Fournier *et al.* one needs a larger value for $\text{Re}f_0$, which can be obtained by choosing $\omega_{\text{eff}} f_{\text{eff}}^2 = -25$ MeV. In the fit this leads to a reduction of $\text{Im}f_0$ and therefore to discrepancies with the total cross section data of Block *et al.* [2] and of Johnson [32]. However, as can be seen from Table I, the normalization factors needed for the differential cross section measured by Block *et al.* are well below 1. It is quite likely that the same normalization factors have to be applied to the total cross section data, which would lead to a reduction of $\approx 20\%$. So, from the low energy data alone a solution with lower total cross section cannot be ruled out. However, a value of $\omega_{\text{eff}} f_{\text{eff}}^2 = -25$ MeV would also increase problems in the description of π^+ - ^4He data at $T_\pi = 110$ MeV, so that more evidence speaks in favor of the solution given here.

Although the χ^2 for the data sets at $T_\pi = 60$ and 75 MeV of Crowe *et al.* [3] is very large, we could not find any systematic error that could explain this. Even in a fit to their data alone the χ^2 per data point could not be improved considerably, so we suppose that the quoted error bars are smaller than they should be.

At energies of $T_\pi = 180$ MeV and above, major contributions to χ^2 come from the large angle data points. Here one can see that the parametrization chosen by us is not sufficient any more to describe finer details of the structure at large angles. However, as we are mainly interested in a consistent description of the forward scat-

tering amplitude and there are still more severe discrepancies within the data, we do not think it necessary to change to another parametrization at this point.

A considerable uncertainty arises from the normalization factors. We already mentioned the inconsistencies between different data sets at low energies. There also is a major difference in the normalization factor of Crowe *et al.* [3] at $T_\pi = 75$ MeV and of Brinkmüller *et al.* [11] at $T_\pi = 90$ MeV. At resonance energies the normalization of the data of Brinkmüller *et al.* and of Binon *et al.* [5] are consistent with each other at forward angles. However, the data of Binon *et al.* tend to be below the data of Brinkmüller *et al.* at large angles, which results in a slightly larger normalization factor in the fit. Above the resonance there is again a large difference in the normalization factors for the data of Brinkmüller *et al.* at $T_\pi = 240$ MeV and of Binon *et al.* at $T_\pi = 220$ and 260 MeV.

The total cross sections measured so far do not help a lot to resolve the discrepancies in the normalization factors as the systematic uncertainties of these data are too large. Our solution is in reasonable agreement with most of the total cross section measurements. An exception is the measurement of Johnson [32] at $T_\pi = 51$ MeV, which is also in contradiction with the data of Block *et al.* [2] at the same energy, and the cross sections measured by Wilkin *et al.* [8] at $T_\pi = 110$ –260 MeV, which are systematically above our values. Note that the normalization factors obtained in our analysis for the differ-

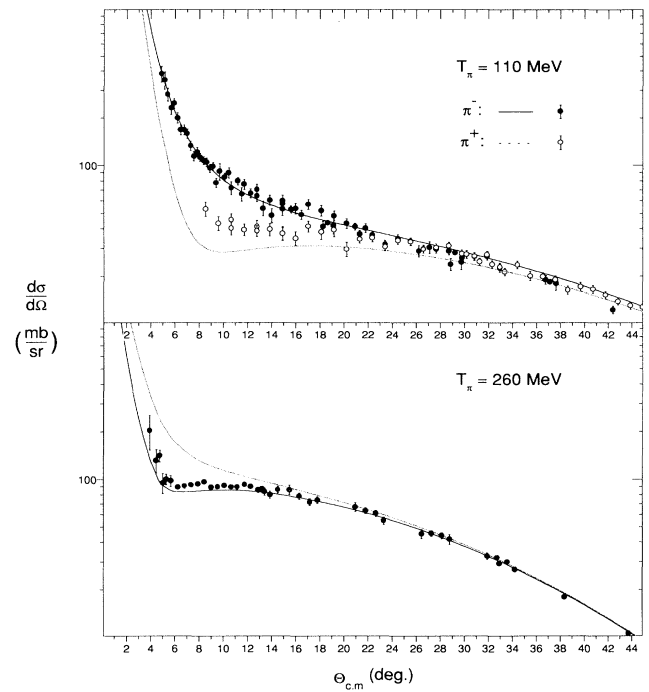


FIG. 7. The Coulomb-nuclear interference region at far forward angles for $T_\pi = 110$ and 260 MeV close to the maxima of $|\text{Re}f_0|$. In both cases the Coulomb-nuclear interference is slightly overpredicted; however, the discrepancy at $T_\pi = 260$ MeV is very small.

ential cross section data at resonance are very close to 1. Furthermore, at $T_\pi = 110$ MeV our solution is in perfect agreement with the value obtained from Binon *et al.* [5] taken as the average value of the total cross sections measured for π^+ and π^- scattering. Unfortunately, this is the only energy where Binon *et al.* measured both π^+ and π^- cross sections. The results obtained at the other energies for π^- only are again systematically above our solution.

The total cross section at the peak of the Δ_{33} resonance strongly influences the calculation of $\text{Re}f_0$ at other energies. Dispersion relation analyses that follow the total cross section data of Wilkin *et al.* overpredict the Coulomb nuclear interference at $T_\pi = 260$ MeV strongly [10]. The new data of π - ^4He scattering at $T_\pi = 110$ MeV [11] reveal additional problems below resonance. The splitting between π^+ and π^- cross section is again smaller than predicted by existing dispersion relation calculations. $\text{Re}f_0$ obtained from our analysis is shown in the bottom part of Fig. 2. The smaller total cross section at resonance results in a reduction of $\text{Re}f_0$ both above and below the resonance and therefore in a smaller splitting between π^+ and π^- cross section.

Figure 7 shows the forward angle region of the data at $T_\pi = 110$ and 260 MeV. These are the most sensitive data for a consistency check with the dispersion relation. All other data sets do not extend far enough into the small angle region or are measured at an energy where the real

part of the forward scattering amplitude and therefore differences due to Coulomb effects between π^+ and π^- scattering are small. A fair description of the data at $T_\pi = 260$ MeV is obtained, with the fit underestimating the data only slightly. However, at $T_\pi = 110$ MeV larger discrepancies remain, especially with the π^+ data, while the description of the π^- data is very good. In a separate fit we verified that a good description of both π^+ and π^- data can be obtained when $\text{Re}f_0$ is reduced further, which requires an even smaller total cross section at resonance.

The reduction of the total cross section at resonance is of great importance for theoretical calculations used to describe π - ^4He scattering. Usually, the π -nucleon scattering amplitude is used as the starting point to calculate π nuclear optical potential. It has been shown that the total cross section depends strongly on effects associated with intermediate nuclear excitations during pion scattering by the same nucleon or by different nucleons [35]. Existing models like the Δ -hole model [36] or microscopic optical models [37] use free parameters to describe the details of the interaction and obtain a good fit to the data. A lower total cross section at resonance could require significant changes of these parameters and the interpretation of the results.

In Table III we give the nuclear phases from our analysis. Because of the inconsistencies between different data sets encountered in our analysis, these results should be used with care. However, we believe that the phases give

TABLE III. Reconstructed phases from the analysis of $^4\text{He}(\pi, \pi)$ scattering.

T_π (MeV)	δ_0 (deg)	δ_1 (deg)	δ_2 (deg)	δ_3 (deg)	δ_4 (deg)	δ_5 (deg)	δ_6 (deg)	δ_7 (deg)
25.0	-4.51	3.12	0.14					
51.0	-8.53	8.80	0.90	0.02				
60.0	-10.01	11.32	1.41	0.05				
68.0	-11.29	13.72	1.98	0.08				
75.0	-12.37	15.89	2.57	0.13				
90.0	-14.58	20.58	4.07	0.27	0.01			
110.0	-17.78	26.38	6.35	0.53	0.03			
130.0	-23.02	30.90	8.36	0.81	0.81	0.06		
150.0	-33.32	33.13	8.98	0.90	0.09	0.01		
180.0	-51.64	23.85	2.53	0.12	0.01	0.00		
220.0	-55.74	-33.44	-16.17	-3.22	-0.65	-0.11	-0.02	
240.0	-54.30	-37.82	-19.63	-5.24	-1.25	-0.25	-0.04	-0.01
260.0	-53.50	-39.49	-20.50	-6.82	-1.89	-0.44	-0.08	-0.01
T_π (MeV)	η_0	η_1	η_2	η_3	η_4	η_5	η_6	η_7
25.0	0.9675	0.9780	0.9984					
51.0	0.9129	0.9426	0.9862	0.9996				
60.0	0.8910	0.9244	0.9760	0.9990				
68.0	0.8701	0.9030	0.9625	0.9981				
75.0	0.8492	0.8794	0.9467	0.9968	0.9999			
90.0	0.7904	0.8124	0.8977	0.9915	0.9996			
110.0	0.6721	0.6870	0.7982	0.9760	0.9984	0.9999		
130.0	0.5200	0.5269	0.6650	0.9470	0.9954	0.9997		
150.0	0.3945	0.3504	0.5155	0.9028	0.9891	0.9991		
180.0	0.3984	0.1165	0.3301	0.8187	0.9709	0.9967	0.9997	
220.0	0.4774	0.1599	0.3384	0.7340	0.9358	0.9889	0.9985	0.9998
240.0	0.4629	0.2350	0.4074	0.7246	0.9214	0.9830	0.9974	0.9997
260.0	0.4311	0.2947	0.4707	0.7342	0.9136	0.9796	0.9962	0.9994

the most consistent description of $\pi\text{-}^4\text{He}$ scattering that can be obtained with the existing data.

To resolve the discrepancies, measurements in the Coulomb-nuclear interference region at far forward angles are needed near $T_{\pi} = 75\text{--}90$ MeV, where the deepest interference minimum is expected for π^{+} scattering. These measurements would also help to solve the problem with the difference in the normalization between the data of Crowe *et al.* and of Brinkmüller *et al.* Further measurements are necessary at energies above the resonance near $T_{\pi} = 300\text{--}400$ MeV again mainly in the forward Coulomb-nuclear interference region. This would determine the forward scattering amplitude at the minimum of its real part.

VI. CONCLUSIONS

Using a phase shift analysis that contains careful treatment of Coulomb effects and the forward dispersion relation we tried to find a consistent description of $\pi\text{-}^4\text{He}$ elastic scattering. Our solution implies that the long standing problem with the real part of the forward scattering amplitude could be due to an overestimation of the total cross section at resonance. The analysis shows clearly which measurements are needed to resolve the remaining discrepancies and to complete the data set for elastic $\pi\text{-}^4\text{He}$ scattering.

The authors are indebted to Prof. E. Boschitz and Prof. H. Pilkuhn for useful discussions.

- [1] M. E. Nordberg, Jr. and K. F. Kinsey, *Phys. Lett.* **20**, 692 (1966).
- [2] M. M. Block, I. Kenyon, J. Keren, D. Koetke, P. Malhotra, R. Walker, and H. Winzeler, *Phys. Rev.* **169**, 1074 (1968).
- [3] K. M. Crowe, A. Fainberg, J. Miller, and A. S. L. Parsons, *Phys. Rev.* **180**, 1349 (1969).
- [4] Yu. A. Shcherbakov, T. Angelescu, I. V. Falomkin, M. M. Kulyukin, V. I. Lyashenko, R. Mach, A. Mihul, N. M. Kao, F. Nichitiu, G. B. Pontecorvo, V. K. Sarychieva, M. G. Sapozhnikov, M. Semerdjieva, T. M. Troshev, N. I. Trosheva, F. Balestra, L. Busso, R. Garfaguini, and G. Piragino, *Il Nuovo Cimento* **31A**, 249 (1976).
- [5] F. Binon, P. Duteil, M. Goua re, L. Hugon, J. Jansen, J.-P. Lagnaux, H. Palevsky, J.-P. Peigneux, M. Spighel, and J.-P. Stroot, *Nucl. Phys.* **A298**, 499 (1978).
- [6] G. Fournier, A. Gerard, J. Miller, J. Picard, B. Saghai, P. Vernin, P. Y. Bertin, B. Coup t, E. W. A. Lingeman, and K. K. Seth, *Nucl. Phys.* **A426**, 542 (1984).
- [7] K. M. Das and B. B. Deo, *Phys. Rev. C* **26**, 211 (1982).
- [8] C. Wilkin, C. R. Cox, J. J. Domingo, K. Gabathuler, E. Pedroni, J. Rohlin, P. Schwaller, and N. W. Tanner, *Nucl. Phys.* **B62**, 61 (1973).
- [9] C. J. Batty, G. T. A. Squier, and G. K. Turner, *Nucl. Phys.* **B67**, 492 (1973).
- [10] W. Grein and M. P. Locher, *J. Phys. G* **6**, 653 (1980).
- [11] B. Brinkm ller, C. L. Blilie, D. Dehnhard, M. K. Jones, G. M. Martinez, S. K. Nanda, S. M. Sterbenz, Yi-Fen Yen, L. G. Atencio, S. J. Greene, C. L. Morris, S. J. Seestrom, G. R. Bureson, K. S. Dhuga, J. A. Faucett, R. W. Garnett, K. Maeda, C. F. Moore, S. Mordechai, A. Williams, S. H. Yoo, and L. C. Bland, *Phys. Rev. C* **44**, 2031 (1991).
- [12] F. Nichitiu, I. V. Falomkin, M. G. Sapozhnikov, Yu. A. Shcherbakov, and P. Piragino, *Il Nuovo Cimento* **67A**, 1 (1982).
- [13] H. Pilkuhn, N. Zovko, and H. G. Schlaile, *Z. Phys. A* **279**, 283 (1976).
- [14] O. Dumbrajs, J. Fr hlich, U. Klein, and H. G. Schlaile, *Phys. Rev. C* **29**, 581 (1984).
- [15] J. Fr hlich, H. G. Schlaile, L. Streit, and H. Zingl, *Z. Phys. A* **302**, 89 (1981).
- [16] J. Fr hlich, H. Pilkuhn, and H. G. Schlaile, *Nucl. Phys.* **A415**, 399 (1984).
- [17] J. Fr hlich, I. Streit, H. Zankel, and H. F. K. Zingl, *J. Phys. G* **6**, 841 (1980).
- [18] J. F. Germond and C. Wilkin, *Ann. Phys. (N.Y.)* **121**, 285 (1979).
- [19] R. F. Frosch, *Phys. Rev.* **160**, 874 (1967).
- [20] J. Fr hlich, H. Pilkuhn, and H. G. Schlaile, *Phys. Lett.* **121B**, 235 (1983).
- [21] H. Pilkuhn, *Relativistic Particle Physics* (Springer, Berlin, 1979).
- [22] J. H fner, L. Tauscher, and C. Wilkin, *Nucl. Phys.* **A231**, 455 (1974).
- [23] T. E. O. Ericson and M. P. Locher, *Nucl. Phys.* **A148**, 1 (1970).
- [24] Ph. Chavanon, M. Crozon, Th. Leray, J. L. Narjoux, and Z. Maric, *Il Nuovo Cimento* **A40**, 935 (1965).
- [25] A. A. Nomoflov, I. M. Sitnik, L. A. Slepets, and L. N. Strunov, *Yad. Fiz.* **18**, 364 (1973) [*Sov. J. Nucl. Phys.* **18**, 187 (1974)].
- [26] T. Ekel f, B. H istad, A.  sberg, C. Busi, S. Dahlgren, A. J. Herz, S. Kullander, G. Lee, D. Websdale, G. Landaud, and J. Yonnet, *Nucl. Phys.* **B35**, 493 (1971).
- [27] V. G. Ableev, A. D. Apokin, A. A. Vorob'ev, G. N. Velichko, Yu. K. Zalite, G. A. Korolev, E. M. Maev, Yu. A. Matulenko, S. B. Nurushev, N. M. Piskunov, V. S. Seleznev, V. V. Siksin, I. M. Sitnik, V. L. Solov'yanov, E. A. Stokovski i, L. N. Strunov, N. K. Terent'ev, A. V. Khanzadeev, V. I. Sharov, and V. A. Shchegel'ski i, *Yad. Fiz.* **34**, 769 (1981) [*Sov. J. Nucl. Phys.* **34**, 428 (1981)].
- [28] B. Badelek, M. Chevallier, G. F ldt, and A. Hallgren, *Phys. Scr.* **29**, 207 (1984).
- [29] D. M. DeMuth and J. S. Chalmers, *Phys. Rev. C* **45**, 353 (1992).
- [30] J. P. Burq, M. Chemarin, M. Chevallier, A. S. Denisov, T. Ekel f, J. Fay, P. Grafstr m, L. Gustafsson, E. Hagberg, B. Ille, A. P. Kashchuk, G. A. Korolev, A. V. Kulikov, M. Lambert, J. P. Martin, S. Maury, J. L. Paumier, M. Querrou, V. A. Schegelsky, I. I. Tkach, M. Verbeken, and A. A. Vorobyov, *Nucl. Phys.* **B187**, 205 (1981).
- [31] J. Boswell, G. S. Das, P. C. Gugelot, J. Kallne, J. McCarthy, L. Orphanos, R. C. Minehart, R. R. Whitney, and P. A. M. Gram, *Nucl. Phys.* **A466**, 458 (1987).
- [32] K. F. Johnson, Ph.D. thesis, New Mexico State University and LAMPF Report LA-6561-T, 1976.
- [33] F. James and M. Roos, *Comput. Phys. Commun.* **10**, 343 (1975).
- [34] M. Kh. Khankhasayev, F. Nichitiu, and M. G. Sapozhnikov, *Czech. J. Phys.* **B36**, 248 (1986).
- [35] M. Wakamatsu, *Nucl. Phys.* **A312**, 427 (1978).
- [36] Y. Horikawa, M. Thies, and F. Lenz, *Nucl. Phys.* **A345**, 386 (1980).
- [37] M. Gmitro, S. S. Kamalov, and R. Mach, *Phys. Rev. C* **36**, 1105 (1987).